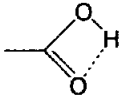


Chapter 3

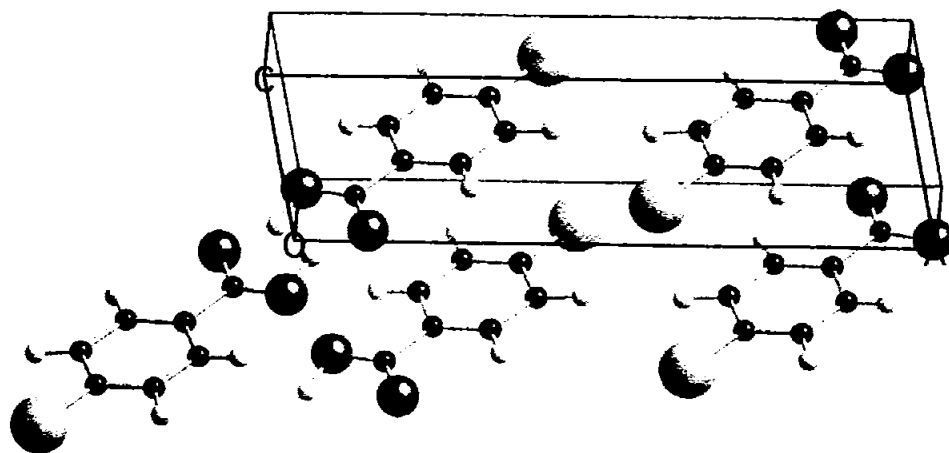
Hydrogen Transfer in Crystalline *p*-Chlorobenzoic Acid

3-1. Introduction

The hydrogen exchange in dimerized benzoic acid in solid has been extensively studied by ^1H NMR [1,2], which enables an accurate description of dynamic behavior of protonic systems. In these studies, the temperature dependence of ^1H NMR spin-lattice relaxation time ($T_{1\text{H}}$) was measured. The observed asymmetric temperature dependence of $T_{1\text{H}}$ (Fig. 1-5) was explained by a two-state jump model described in Chapter 1. *p*-Chlorobenzoic acid was also reported to make a dimer structure[3] analogous to benzoic acid [4] in solid as shown in Fig. 3-1, and the presence of the simultaneous double H-jumps between two potential wells was shown by Nagaoka *et. al.*, using the ^1H NMR method [1,2]. The X-ray diffraction study of *p*-chlorobenzoic acid [3] showed a short hydrogen bonded O—H \cdots O distance of 2.615 (5) Å, and the position of the hydrogen atom in hydrogen bonding is disordered. The six carbon atoms in the benzene ring are coplanar, and the best plane through the four atoms of the carboxyl group makes an angle of 5.7 ° with the plane of the benzene ring [3]. This result indicates that a π -electron system is made from the carboxyl group to the chlorine atom through a phenyl ring. The dimer planes form one-dimensional

stacking along the crystallographic *c* axis. Since the nearest Cl \cdots H—O distance of *ca* 5 Å is obtained in the same molecule[3], no Cl \cdots H—O intramolecular hydrogen bond is expected. Considering the structure studied by the X-ray diffraction [3] as shown in Figure 3-1, intramolecule hydrogen bond  is little and a *p*-chlorobenzoic acid dimer is isolated from neighboring dimers except one-dimensional stacking along the crystallographic *c* axis. A *p*-chlorobenzoic acid dimer is located on an inversion center in crystals indicating that two hydrogen bonds in a dimer are equivalent.

In this chapter, we want to show how sensitively the NQR technique can be applied to the study of the H-motion compared with the ^1H NMR method. Along this purpose we measured ^{35}Cl NQR frequencies and spin-lattice relaxation time in *p*-chlorobenzoic acid and its partially deuterated analog.



Space group	$P\bar{1}$
Lattice parameters	$a = 14.392$ $b = 6.227$ $c = 3.861$ Å
	$\alpha = 88.86^\circ$ $\beta = 100.12^\circ$ $\gamma = 93.31^\circ$
	$Z = 2$

Figure 3-1. The crystal structure of PCBA acid determined by X-ray diffraction at room temperature [3].

3-2. Experimental

Crystalline *p*-Chlorobenzoic acid, $p\text{-ClC}_6\text{H}_4\text{CO}_2\text{H}$ (abbreviated to PCBA) was obtained by recrystallization of the commercial reagent from acetone. Colorless, and needle crystals of PCBA were obtained by cooling an acetone solution from 50°C down to room temperature. A partially deuterated analog $p\text{-ClC}_6\text{H}_4\text{CO}_2\text{D}$ (PCBA- d_1) was prepared by repeated crystallizations of the protonated compound from CH_3OD .

The ^{35}Cl NQR frequencies in both PCBA and PCBA- d_1 were measured with a homemade pulsed spectrometer described in Chapter 2 [5] in a temperature range 77-140 K. Free induction decays after a 90° pulse were observed to determine ^{35}Cl NQR frequencies. The ^{35}Cl NQR spin-lattice relaxation time (T_{1Q}) in both analogs were measured in a range 77-140 K.

The ^1H NMR spin-lattice relaxation time T_{1H} in PCBA was measured with a homemade spectrometer shown in Chapter 2 [6] at a Larmor frequency of 54.3 MHz in a temperature range 30-300 K using the saturation recovery method.

3-3. Results

3-3-1. ^{35}Cl NQR Frequencies

Temperature dependences of ^{35}Cl NQR frequencies observed in PCBA and PCBA- d_1 are shown in Figure 3-2. PCBA and PCBA- d_1 gave a single resonance line at 34.673 ± 0.001 and 34.674 ± 0.002 MHz, respectively at 77 ± 1 K. The observed frequency of 34.673 MHz in PCBA at 77 K agrees well with the reported value of 34.673 MHz [7]. Resonance frequencies and temperature dependences observed in both compounds were quite analogous in the whole temperature range studied and the frequency difference in the two compounds observed at 130 K was 2.5 kHz. Upon heating, resonance signals in both compounds were gradually weakened, and disappeared in the noise level around 140 K.

3-3-2. ^{35}Cl NQR Spin-Lattice Relaxation Time (T_{10})

Temperature dependences of ^{35}Cl NQR T_{10} observed in PCBA and PCBA- d_1 are shown in Figure 3-3. A shallow minimum of 8.0 ± 1.0 ms was observed at *ca.* 110 K in PCBC, while a deep minimum of 0.80 ± 0.10 ms was obtained at *ca.* 130 K in PCBA- d_1 .

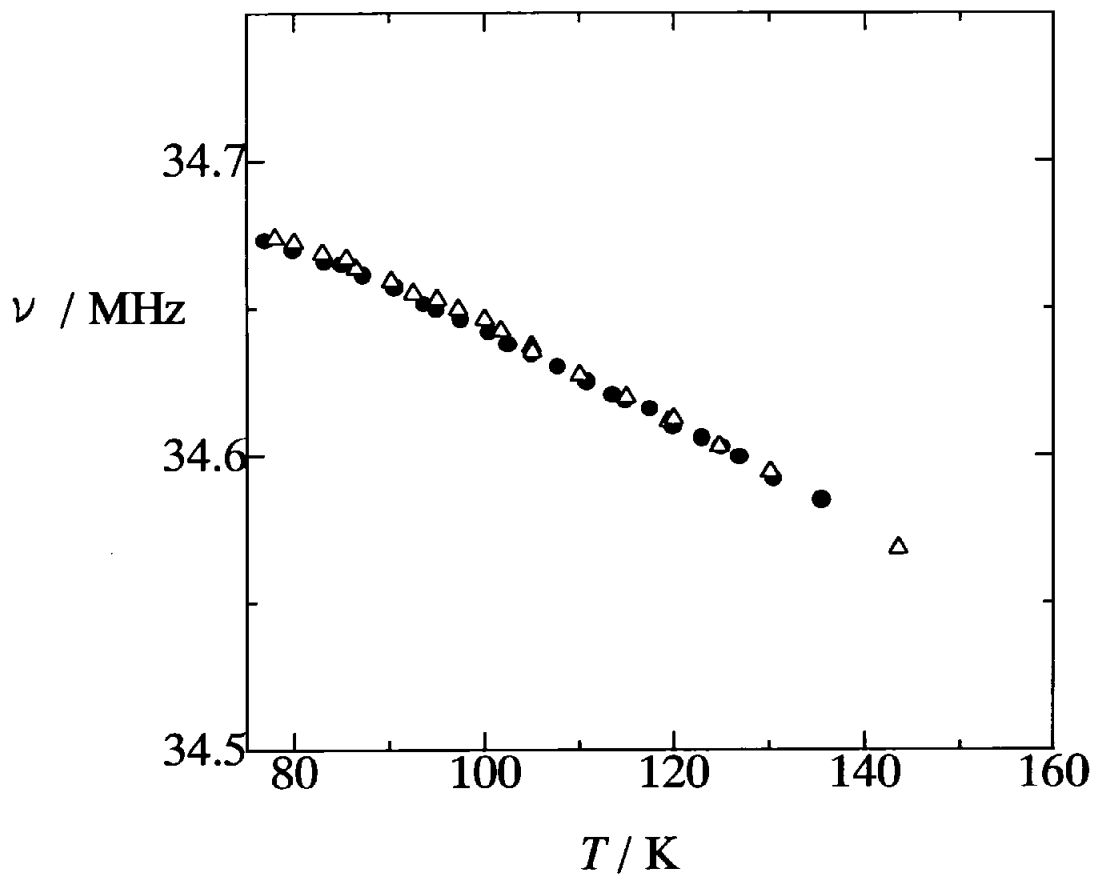


Figure 3-2. Temperature dependences of ^{35}Cl NQR frequencies (ν) observed in $p\text{-ClC}_6\text{H}_4\text{CO}_2\text{H}$ (PCBA) (●) and $p\text{-ClC}_6\text{H}_4\text{CO}_2\text{H}$ (PCBA- d_1) (△).

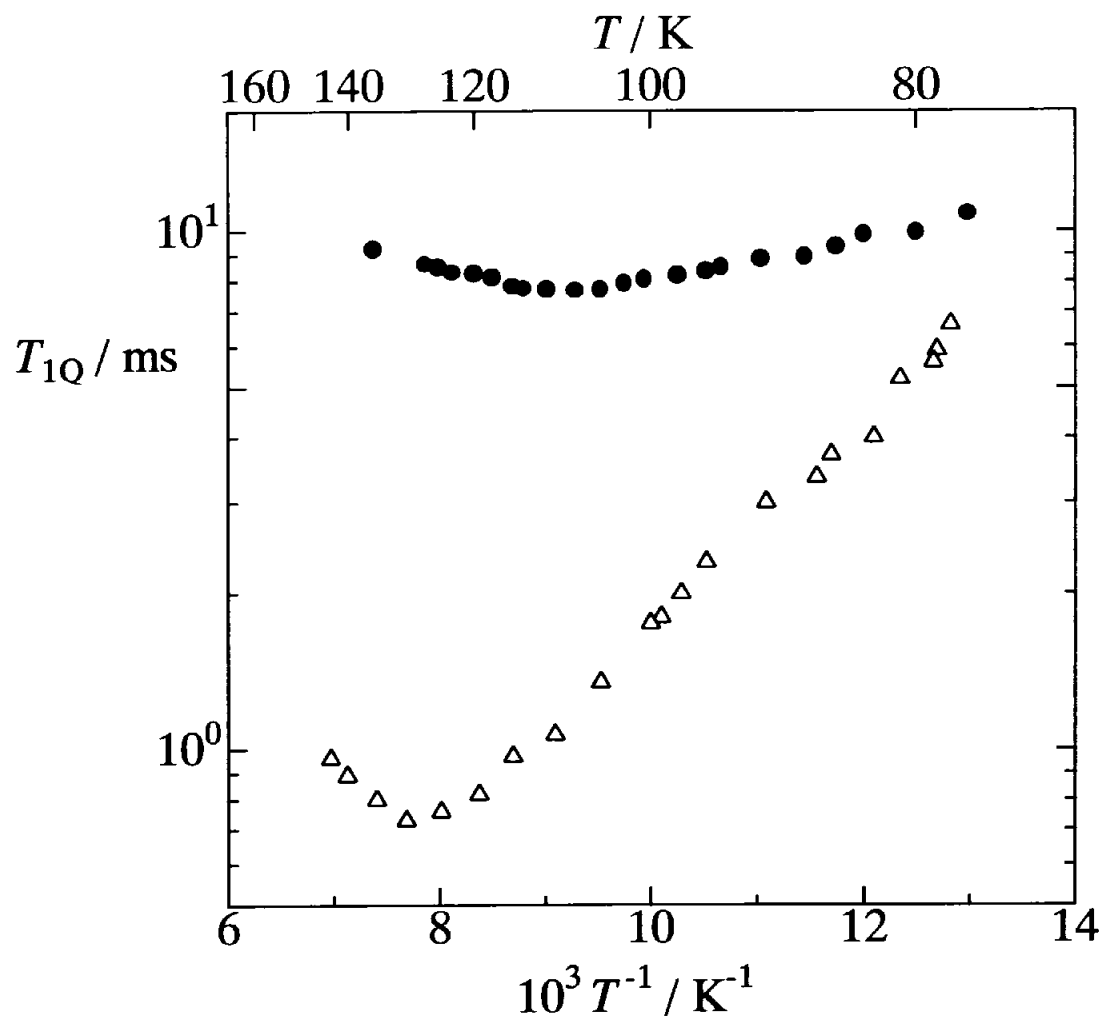


Figure 3-3. Temperature dependences of the ^{35}Cl NQR spin-lattice relaxation times T_{1Q} observed in $p\text{-ClC}_6\text{H}_4\text{CO}_2\text{H}$ (PCBA) (●) and $p\text{-ClC}_6\text{H}_4\text{CO}_2\text{H}$ (PCBA- d_1) (△).

3-3-3. ¹H NMR Spin-Lattice Relaxation Time (T_{1H})

A temperature dependence of ¹H NMR T_{1H} observed in PCBA at 54.3 MHz is shown in Figure 3-4, where data observed in the high-temperature range reported by Nagaoka *et. al.* [1,2] at a Larmor frequency of 59.53 MHz are shown. Our results are close to their data, but the agreement was not satisfactory. Their T_{1H} values shorter than ours seem to be attributed to short pulse repetition times in their measurement because of quite long T_{1H} values in this compound. An asymmetric T_{1H} curve with a minimum at *ca.* 105 K was clearly observed.

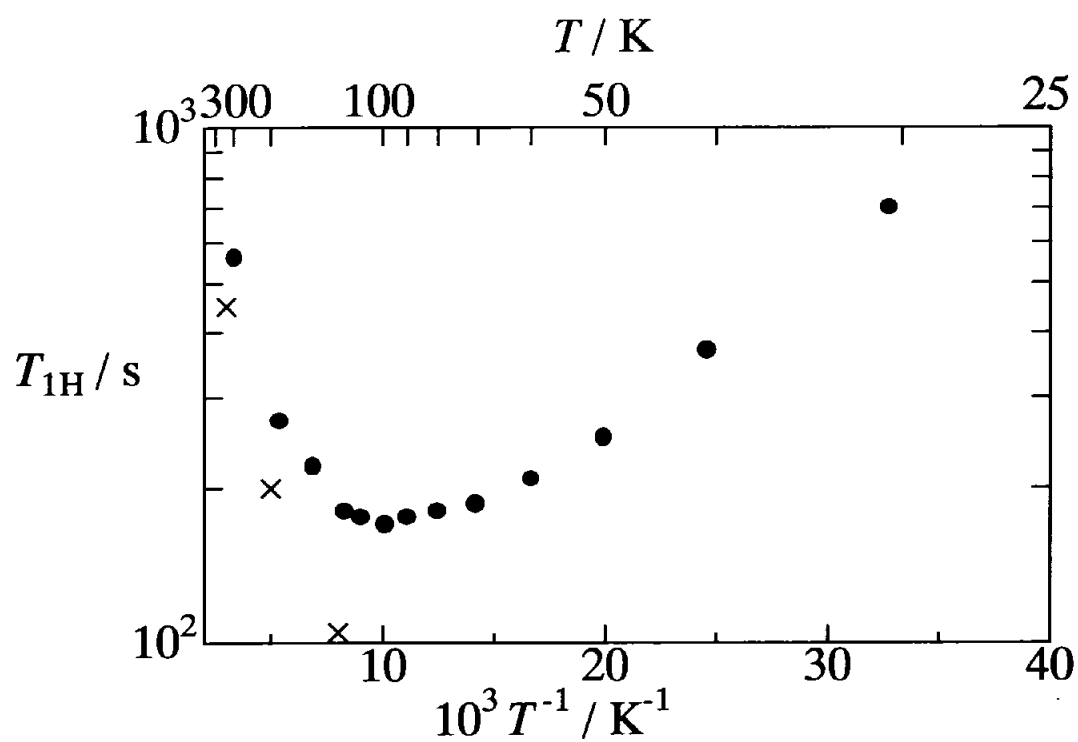


Figure 3-4. Temperature dependences of the ^1H NMR spin-lattice relaxation time $T_{1\text{H}}$ observed in in $p\text{-ClC}_6\text{H}_4\text{CO}_2\text{H}$ (PCBA) at a Larmor frequency of 54.3 MHz (●) and 59.53 MHz (×) reported by Nagaoka *et. al.* [1].

3-4. Discussion

3-4-1. ¹H NMR Spin-Lattice Relaxation Time (T_{1H})

The asymmetric temperature dependence of T_{1H} observed in PCBA shown in Fig. 3-4 is quite analogous to T_{1H} reported for crystalline benzoic acid (BA) [1,2] in which the double proton transfer between the hydrogen bonded two molecules, as illustrated in Figure 3-5, was shown to contribute to this relaxation. The observed temperature dependence of T_{1H} in PCBA shown in Fig. 3-4 is similar to that in BA in the asymmetric shape, and the position of the minimum. We can, accordingly, expect that relaxation mechanisms in PCBA and BA are the same. Referring to the analysis of T_{1H} observed in BA [1,2], the steep temperature dependence observed in the high-temperature side of the minimum can be explained by the BPP type relaxation [8] due to the classical random hydrogen jumps in an asymmetric double-well potential formed in the dimer structure. On the other hand, the relaxation in the low-temperature side is attributed to the quantum mechanical proton tunneling coupled to crystalline phonons [5]. The asymmetry double-well potential model assumed in the present analysis is shown in Figure 3-6. We analyzed the obtained T_{1H} data using the same theoretical treatment as performed on BA given by

$$T_{1H}^{-1} = C \frac{a}{(1+a)^2} \left[\frac{\tau_c}{1+(\omega\tau_c)^2} + \frac{4\tau_c}{1+4(\omega\tau_c)^2} \right], \quad (3.1)$$

and

$$a = \exp(A/RT). \quad (3.2)$$

Eqs. (3.1) and (3.2) give the BPP type relaxation in an asymmetric double-well potential shown in Fig. 3-6. C is a constant, ω is the Larmor frequency, and A is the potential energy difference given by $A = E_1 - E_2$, where E_1 and E_2 are activation barriers from sites 1 and 2, and τ_c is the overall correlation time for the motion in the asymmetric double-well potential defined by

$$\frac{1}{\tau_c} = k_{12} + k_{21}, \quad (3.3)$$

where k_{12} is the rate constant for the $1 \rightarrow 2$ transition, while the reverse rate constant k_{21} is given by

$$k_{21} = k_{12}a. \quad (3.4)$$

At high temperatures, since the quantum mechanical proton tunneling can be ignored, the high temperature rate constants k_{12}^H and k_{21}^H can be written by the Arrhenius form for the activated barrier crossing.

$$k_{12}^H = \frac{1}{\tau_0} \exp(-V/RT) \quad (3.5)$$

and

$$k_{21}^H = \frac{1}{\tau_0} = \exp[-(V - A)/RT], \quad (3.6)$$

where V is the barrier height shown in Figure 3-6.

Since the quantum mechanical proton tunneling process is major for the relaxation at low temperatures, the low temperature rate constants k_{12}^L and k_{21}^L derived by J. L. Skinner and H. P. Trommsdorff [9] are expressed as

$$k_{12}^L = k_0 n(A) \quad (3.7)$$

and

$$k_{21}^L = k_0 [n(A) + 1], \quad (3.8)$$

where $n(A)$ is defined by

$$n(A) = \frac{1}{\exp(A/RT) - 1}. \quad (3.9)$$

On the other hand, at intermediate temperatures, the relaxation mechanism is related with not only the classical random jump but also the quantum mechanical proton tunneling. The rate constants k_{12} and k_{21} at intermediate temperatures, therefore, are shown to be given by

$$k_{12} = k_{12}^L + k_{12}^H \quad (3.10)$$

and

$$k_{21} = k_{21}^L + k_{21}^H. \quad (3.11)$$

We fitted Eqs. (3.1)-(3.11) to the data shown in Fig. 3-4, where C in Eq. (3.1) expressing the magnetic dipolar interaction modulated by this proton transfer was estimated from the C value reported for BA, where we assumed that the ratio of C in the two compounds is roughly equal to that of the observed T_{1H} minimum values. This is because no data on H positions in crystals are available in PCBA. The obtained best fitted T_{1H} curve and determined parameters are shown in Fig. 3-7 and Table 3-1, respectively.

k_0 of $2.0 \times 10^{10} \text{ s}^{-1}$ obtained in PCBA larger than $4.5 \times 10^8 \text{ s}^{-1}$ in BA indicating that the tunneling in PCBA is more marked than in BA, is explainable by a stronger hydrogen bonding in PCBA with a short O---O distance of 2.615 Å [3] compared with 2.64 Å in BA [4, 10, 11]. This difference comes from more acidic protons in PCBA due to the electron attracting effect of chlorine. The remarkable difference in T_{1H} minimum values in PCBA (78 s at 54.3 MHz) and BA (*ca.* 6s at 59.53 MHz [1,2]) implies that the H displacement in the double proton transfer process in PCBA is smaller than in BA. This can also be explained by the difference in the O---O separations or the strength of hydrogen bonding in the two carboxylic acids.

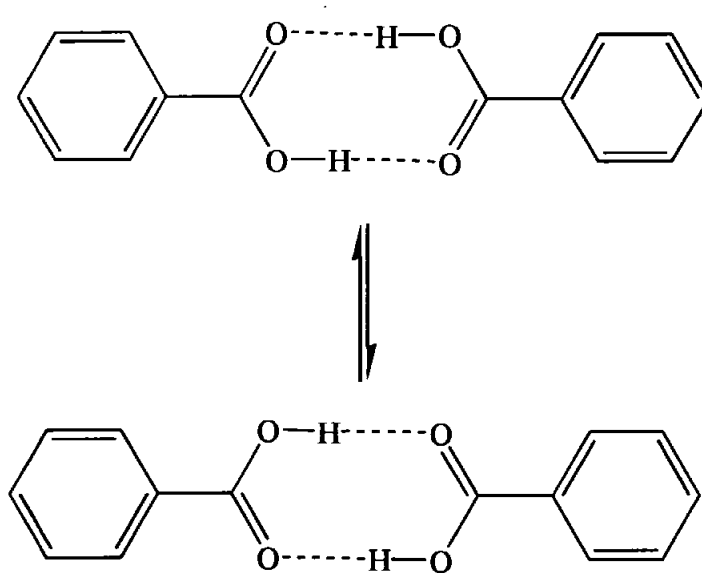


Figure 3-5. The double hydrogen transfer model. Two hydrogen atoms in the carboxylic acid dimer jump at the same time.

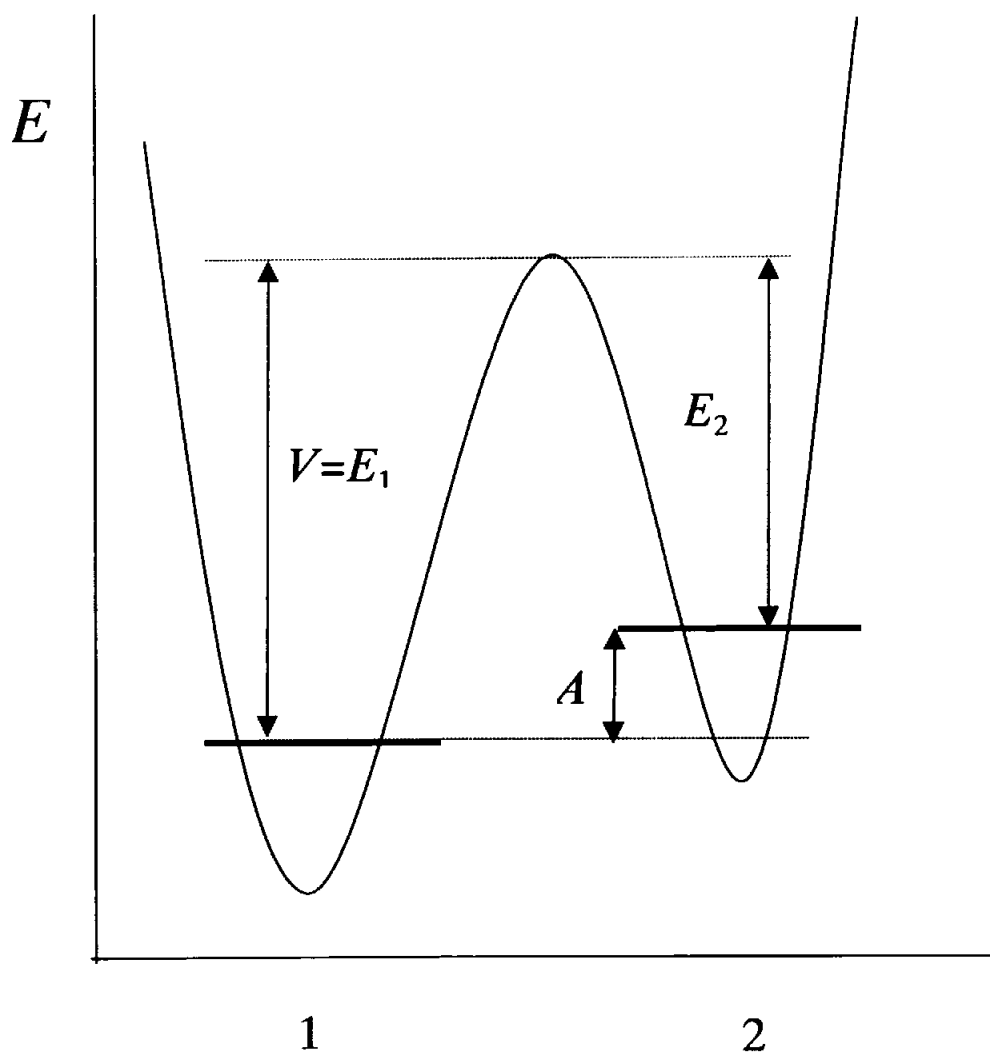


Figure. 3-6. An asymmetric double minimum potential curve for hydrogen transfer model. A denotes the potential energy difference, and V denotes the barrier height. The horizontal axis shows the interaction coordinate.

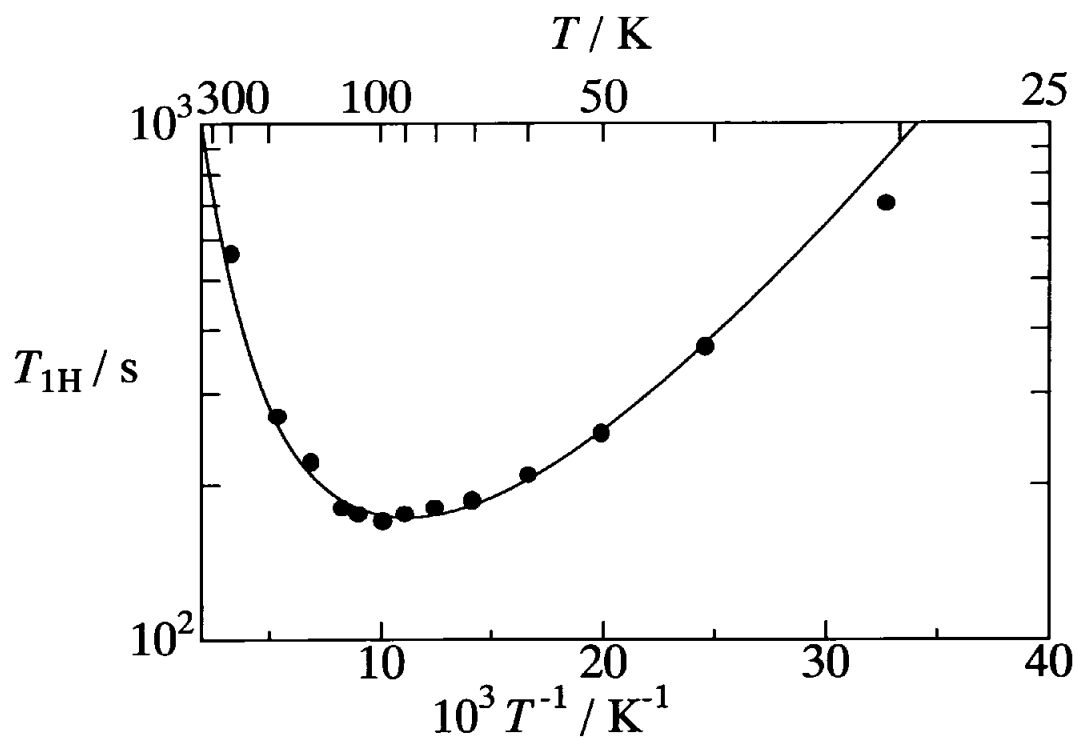


Figure 3-7. A comparison between the observed and calculated temperature dependences of the ^1H NMR spin-lattice relaxation time $T_{1\text{H}}$. The solid curve is best-fitted by using Eqs. (3.1)-(3.11) including the quantum mechanical proton tunneling coupled to crystalline phonons and the classical H-jumping.

Table 3-1. Motional parameters of the proton transfer in carboxylic acid dimers determined in *p*-chlorobenzoic acid from ^1H NMR relaxation data together with the reported values in benzoic acid.

	$V / \text{kJ mol}^{-1}$	τ_0 / s	$A / \text{kJ mol}^{-1}$	k_0 / s^{-1}	C / s^{-2}
<i>p</i> -chlorobenzoic acid (PCBA)	8 ± 2	1.3×10^{-12}	0.98 ± 0.2	2.0×10^{10}	2.40×10^7
benzoic acid (BA) ^[6]	5.5	3.3×10^{-12}	0.72	4.5×10^8	2.84×10^8

3-4-2. ³⁵Cl NQR Frequencies

³⁵Cl NQR frequencies observed above 77 K in both PCBA and PCBA-*d*₁ shown in Figure. 3-2.

In most cases, NQR frequency is decreased with the temperature increase and this decrease is explained by the Bayer theory [12], which takes into account the averaging electric field gradient (efg) at resonant nuclei by lattice and molecular vibrations. According to this theory, the temperature dependence of NQR frequency is given by [12]

$$\nu(T) = \nu(0) - \frac{3}{8\pi^2} \frac{h\nu_Q}{I_t\nu_t} \frac{1}{\exp(h\nu_t/kT) - 1}, \quad (3.12)$$

and

$$\nu(0) = \nu_Q \left(1 - \frac{3}{16\pi} \frac{h}{I_t\nu_t} \right), \quad (3.13)$$

where $\nu(0)$ is the NQR frequency at 0 K, ν_Q is the NQR frequency without the zero point vibration, ν_t is the frequency of the rotational lattice vibration affecting efg average, and I_t is the moment of inertia for the vibration mode.

In case the temperature is not high enough and the lattice vibrations are assumed to be harmonic, the temperature dependence of NQR frequency can be roughly expressed by a linear relation with temperature, and is approximately given by

$$\nu(T) = \nu(0) - CT \quad (3.14).$$

In the present study, the temperature dependence of frequencies observed in both PCBA and PCBA-*d*₁ could be explained well by Eq. (3.14) up to the temperature of the signal disappearance observed around 140 K. This implies no marked unharmonic molecular motions averaging efg and also the absence of phase transitions.

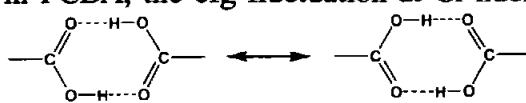
It is noted that the two analogs showed almost the same frequencies in the whole temperature range studied. This suggests that the averaged efg at Cl nuclei is almost unaffected by the deuteration in the carboxyl group.

3-4-3. ³⁵Cl NQR Spin-Lattice Relaxation Time (*T*_{1Q})

The obtained results that *T*_{1Q} in PCBA gave a minimum at almost the same temperature of *ca.* 105 K as that of *T*_{1H}, and also the slope of *T*_{1Q} of *ca.* 0.78±0.3 kJ mol⁻¹ in the low-temperature side of the minimum shown in Fig. 3-8 is close to 0.98±0.2 kJ mol⁻¹ in *T*_{1H}, indicate that the relaxation mechanisms in *T*_{1Q} and *T*_{1H} are the same, *i.e.*, the double proton transfer in the dimer. It is noted that a marked difference between PCBA and PCBA-*d*₁ was observed in *T*_{1Q} temperature dependences shown in Fig. 3-3, where a shallow minimum of *ca.* 8.0±1.0 ms was observed in PCBA around the same temperature of *ca.* 105 K as that in the *T*_{1H} minimum, while a deep minimum of 0.80±0.10 ms in PCBA-*d*₁ at *ca.* 130 K higher than that in PCBA. This indicates that the observed *T*_{1Q} temperature dependence is closely connected with the hydrogen transfer process in carboxylic acid dimers. The markedly smaller *T*_{1Q} values obtained in NQR

than in NMR imply that the hydrogen transfer in these systems can be observed much more sensitively in NQR than in NMR studies.

An interesting result in T_{1Q} data is that the deuterated and undeuterated analogs exhibited quite different T_{1Q} behavior from each other, even though they showed quite analogous resonance frequencies in a wide temperature range. An important characteristic of hydrogen transfer in PCBA- d_1 is the tunneling splitting much smaller than that in PCBA because of the marked mass effect on tunneling which results in quite small tunneling probability in deuterated systems [13]. If we can ignore the contribution from the tunneling to T_{1Q} in the deuterated analog, the steep T_{1Q} slope observed in the low-temperature side of the minimum is explainable mostly by the classical H-jumps. The T_{1Q} minimum temperature in PCBA- d_1 higher than that in PCBA can be understood by the shorter O—D, that is a longer O---O distance in the deuterated dimer so-called the Ubbelohde effect [14, 15, 16, 17], shown in Fig.3-9, resulting in the D-jumping rate slower than that of the H-motion.

A remarkable difference in T_{1Q} observed in the two analogs is their minimum values, *i.e.*, that in PCBA- d_1 is about ten times shorter than in PCBA. This can be explained by considering the tunneling which makes quantum mechanical proton delocalization by overlapping two protonic wave functions implying that the tunneling process is not a motion but a state giving no marked fluctuation of the electric field gradient(efg) Since, in PCBA, the efg fluctuation at Cl nuclei at high temperatures made by the exchange  is partly averaged by the tunneling, the effective fluctuation in PCBA occurring around the T_{1Q} minimum is expected to be smaller than in the deuterated analog with the markedly diminished tunneling.

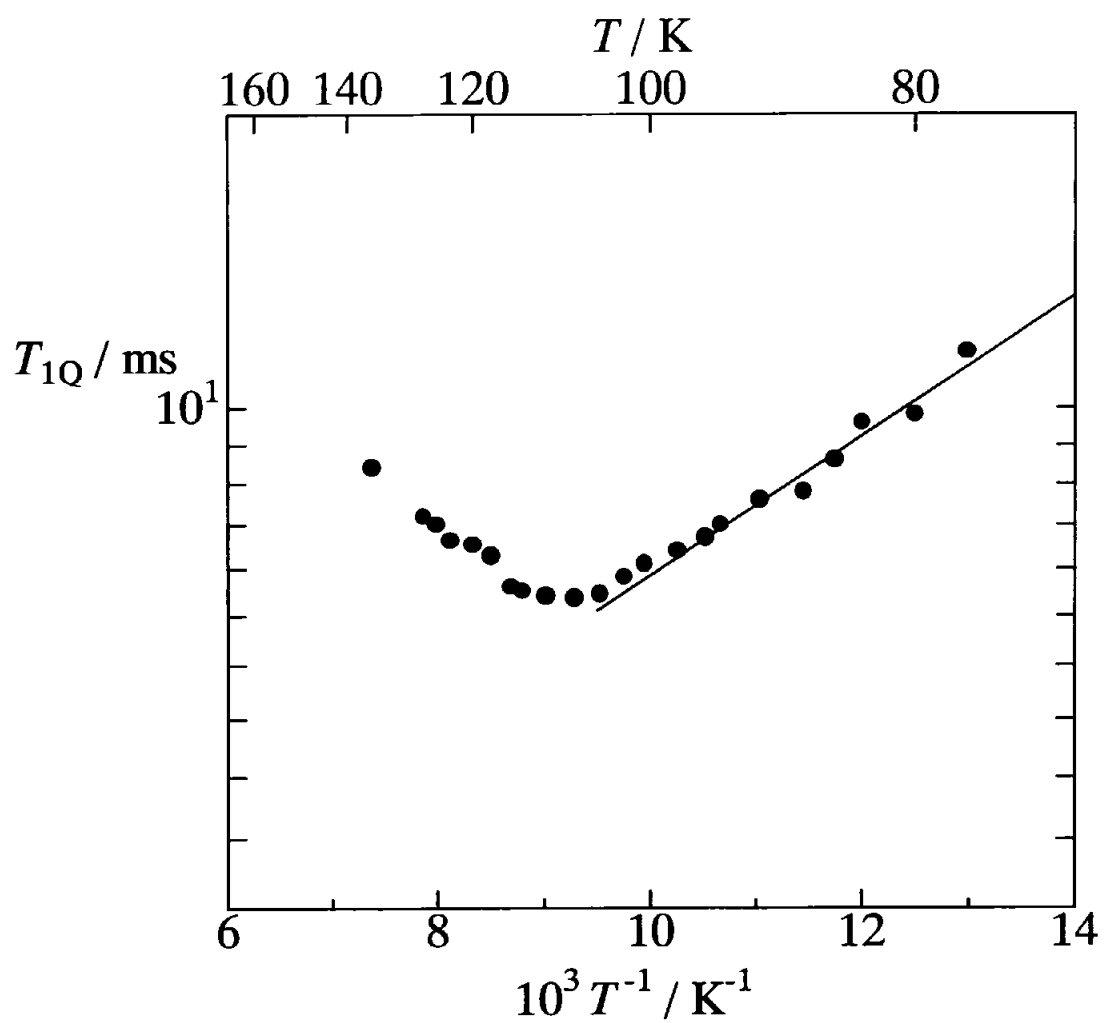


Figure 3-8. Analysis of the temperature dependence of the ^{35}Cl NQR T_{10} observed in PCBA. Solid line is drawn to obtain the activation energy.

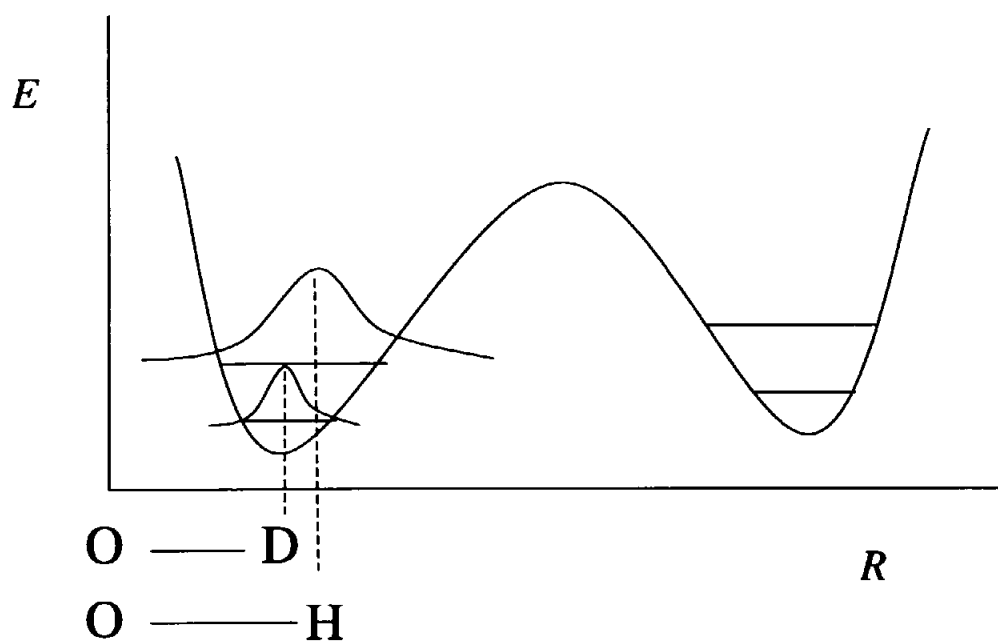


Figure 3-9. The Ubbelohde effect exhibiting the difference between O—H---O and O—D---O hydrogen bonds. Deuterated analog PCBA- d_1 has a weaker hydrogen bond than that of PCBA, because the zero-point vibration energy in deuterated PCBA- d_1 is lower than in PCBA.

References

- [1] S. Nagaoka, T. Terao, F. Imashiro, A. Saika, and N. Hirota, *J. Chem. Phys.*, **79**, 4694 (1983).
- [2] S. Nagaoka, T. Terao, F. Imashiro, A. Saika, N. Hirota, and S. Hayashi, *Chem. Phys. Lett.*, **80**, 580, (1981).
- [3] R. S. Miller, I.C.Paul, and D. Y. Curtin, *J. Am. Chem. Soc.*, **96**, 6334 (1974).
- [4] G. A. Sim, J. M. Robertson, and T. H. Goodwin, *Acta Cryst.*, **8**, 157 (1955).
- [5] H. Miyoshi, K. Horiuchi, N. Sakagami, K. Okamoto, and R. Ikeda, *Z. Naturforsch.*, **53a**, 603 (1998).
- [6] T. Kobayashi, H. Ohki, and R. Ikada, *Mol. Cryst. Liq. Cryst.*, **257**, 279(1994).
- [7] H. C. Meal, *J. Am. Chem. Soc.*, **74**, 6121 (1952).
- [8] A. Abragam, *The Principles of Nuclear Magnetism*, Oxford university Press, New York 1986, Chapt VIII.
- [9] J. L. Skinner, and H.P. Trommsdorff, *J. Chem. Phys.*, **89**, 897 (1988).
- [10] G. Bruno, L. Randaccio, *Acta Cryst.*, **B36**, 1711(1980).
- [11] R. Feld, M. S. Lehmann, K. W. Muir, J. C. Speakman, *Z. Kristallogr.*, **157**, 215(1981).
- [12] H. B. Bayer, *Z. Physik.*, **130**, 227 (1951).
- [13] A. Stökli, B. H. Meier, R. Meyer, and R. R. Ernst, *J. Chem. Phys.*, **93**, 1502 (1990).
- [14] J.M. Robertson, and A. R. Ubbelohde, *Proc. Roy. Soc. A*, **170**, 222 (1939).
- [15] J.M. Robertson, and A. R. Ubbelohde, *Proc. Roy. Soc. A*, **170**, 241 (1939).
- [16] A. R. Ubbelohde, *Proc. Roy. Soc. A*, **173**, 417 (1939).
- [17] A. R. Ubbelohde, and I. Woodward, *Proc. Roy. Soc. A*, **179**, 399 (1942).